Angular Dispersion and Deflection Function for Heavy Ion Elastic Scattering *

BAI Zhen(白真)[1,2], WANG Qi(王琦)[1**], HAN Jian-Long(韩建龙)[1,2], XIAO Zhi-Gang(肖志刚)[1], XU Hu-Shan(徐瑚珊)[1], SUN Zhi-Yu(孙志宇)[1], HU Zheng-Guo(胡正国)[1,2], ZHANG Xue-Ying(张雪荧)[1,2], WANG Hong-Wei(王宏伟)[1], MAO Rui-Shi(毛瑞士)[1], YUAN Xiao-Hua(袁小华)[1,2], XU Zhi-Guo(徐治国)[1], ZHANG Hong-Bin(张宏斌)[1], XU Hua-Gen(徐华根)[1,2], QI Hui-Rong(祁辉荣)[1,2], WANG Yue(王玥)[1,2], JIA Fei(贾飞)[1,2], WU Li-Jie(武丽杰)[1,2], DING Xian-Li(丁先利)[1,2], GAO Qi(高启)[1,2], GAO Hui(高辉)[1,2], LI Song-Lin(李松林)[1], LI Jun-Qing(李君清)[1], ZHANG Ya-Peng(张亚鹏)[1,2], XIAO Guo-Qing(肖国青)[1], JIN Gen-Ming(靳根明)[1,3], REN Zhong-Zhou(任中洲)[3,4], ZHOU Shan-Gui(周善贵)[5], XU Wang(徐望)[6], Fan Gong-Tao(范功涛)[6], ZHANG Shuang-Quan(张双全)[7], PANG Dan-Yang(庞丹阳)[7], SERGEY Yu-Kun[8,9]

[1]*Institute of Modern Physics, Chinese Academy of Sciences, Lanzhou 730000*
[2]*Graduate University, Chinese Academy of Sciences, Beijing 100039*
[3]*Center of Theoretical Nuclear Physics, National Laboratory of Heavy-Ion Accelerator, Lanzhou 730000*
[4]*Department of Physics, Nanjing University, Nanjing 210093*
[5]*Institute of Theoretical Physics, Chinese Academy of Sciences, Beijing 100080*
[6]*Shanghai Institute of Applied Physics, Chinese Academy of Sciences, Shanghai 201800*
[7]*Department of Technical Physics, Peking University, Beijing 100871*
[8]*Centro de Ciencias Físicas, National University of Mexico (UNAM), Cuernavaca, Mexico*
[9]*Center for Nonlinear Physics, RSPhysSE, The Australian National University, Canberra ACT 0200, Australia*

(Received 15 August 2007)

The differential cross sections for elastic scattering products of ^{17}F on ^{208}Pb have been measured. The angular dispersion plots of $\ln(d\sigma/d\theta)$ versus θ^2 are obtained from the angular distribution of the elastic scattering differential cross sections. Systematical analysis on the angular dispersion for the available experimental data indicates that there is an angular dispersion turning angle at forward angular range within the grazing angle. This turning angle can be clarified as nuclear rainbow in classical deflection function. The exotic behaviour of the nuclear rainbow angle offers a new probe to investigate the halo and skin phenomena.

PACS: 25.60.Bx, 25.60.Dz, 25.70.Bc

Elastic scattering is a basic process in nuclear collisions because it accompanies another reaction mechanism, and a thorough understanding of elastic scattering is a prerequisite for a valid description of non-elastic processes. In heavy ion collisions, the wavelength of relative motion is small as compared to the characteristic lengths of the interaction potential. Therefore, heavy ion collisions can frequently be treated in the classical limit. The classical deflection function is a basic and fruitful tool for describing elastic scattering in heavy ion collisions.[1−3]

In this Letter, the experimental data of elastic scattering differential cross section of weakly bound nucleus ^{17}F on ^{208}Pb target are presented and analysed. We find that the fitting of the experimental angular dispersion plot $\ln(d\sigma/d\theta)$ versus θ^2 of elastic scattering products is out of line, there is a turning point with two different slopes at small angle. The turning point corresponds to a cross section singularity in the classical deflection function. It is clarified as a nuclear rainbow angle. The exotic behaviour of the nuclear rainbow angle provide a new probe to identify the abnormal structure of weakly bound nuclei.

The experiment was performed[4] with the Radioactive Ion Beam Line in Lanzhou (RIBLL) at the Institute of Modern Physics, Chinese Academy of Sciences, Lanzhou. The differential cross sections $(d\sigma/d\theta)$ have been measured at forward angular range $\theta_{\rm lab}$ from 6° to 20° for the elastic scattering products of ^{17}F and ^{17}O induced from the reactions of ^{17}F+^{208}Pb at 141 MeV and ^{17}O+^{208}Pb at 128 MeV, respectively. The angular dispersion plots of $\ln(d\sigma/d\theta)$ versus θ^2 are plotted in Fig. 1 for ^{17}F and ^{17}O. Two different behaviours are obviously presented. In order to fit the experimental data, two straight lines with different slopes for the weakly bound products ^{17}F are needed, but only one straight line for the stable nucleus ^{17}O in the same angular range.

In heavy ion peripheral collisions an expression of angular dispersion has been suggested by Strutinsky[5] and it is widely used in the analysis of experimental data.[6−12] The differential cross section $(d\sigma/d\theta)$ at a small angular range can be formulated as

$$\frac{d\sigma}{d\theta} \propto e^{-[(\theta-\theta_0)/\xi]^2} + e^{-[(\theta+\theta_0)/\xi]^2}. \qquad (1)$$

For a peak-forward angular distribution, there is $\theta_0 =$

*Supported by the National Natural Science Foundation of China under Grant Nos 10675149 and 10535010, the Chinese Academy of Sciences under Grant No KJCX3.SYW.N1, and the National Basic Research Programme of China under Grant No 2007CB81500.

**Email: wangqi@impcas.ac.cn

0, and then Eq. (1) reduces to

$$\frac{d\sigma}{d\theta} \propto e^{-(\theta/\xi)^2}. \quad (2)$$

In Eq. (2), the logarithm of the differential cross section $\ln(d\sigma/d\theta)$ is a linear function of the square of the scattering angle θ^2. Both the quantities of the differential cross section $(d\sigma/d\theta)$ and the scattering angle θ can be directly measured in an experiment. In the plane of $\ln(d\sigma/d\theta)$ vs θ^2, the slope represents the so-called angular dispersion parameter ξ. The angular dispersion ξ is determined by both the quantal dispersion coefficient ξ_q and the dynamic quantity ξ_r,

$$\xi = (\xi_q^2 + \xi_r^2)^{1/2}. \quad (3)$$

For a pure Rutherford scattering, the nuclear interaction and then the dynamic angular dispersion is negligible, there is only quantal angular dispersion. However, there are both quantal angular dispersion and dynamic angular dispersion due to nuclear interaction in heavy ion elastic scattering. This is a very important different behaviour, there is a sole slope for the pure Rutherford scattering without the nuclear reaction, and there is another different slope for the elastic scattering including the nuclear reaction. As soon as there has been an evolution from a pure Rutherford scattering to elastic scattering including the nuclear reaction, there is a slope change in the angular dispersion plot of $\ln(d\sigma/d\theta)$ vs θ^2.

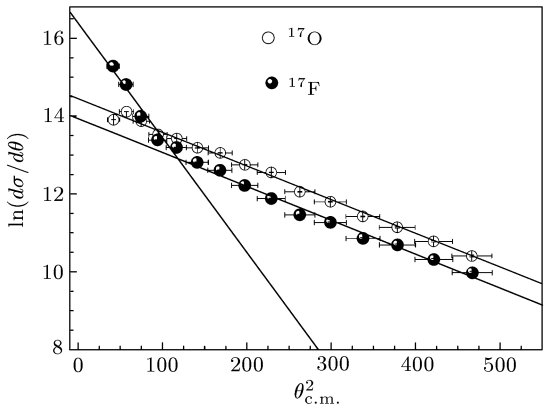

Fig. 1. Angular dispersion plots $\ln(d\sigma/d\theta)$ vs θ^2 of elastic scattering $^{17}F/^{17}O$ on target ^{208}Pb.

In order to test and to verify our experimental results, we collect the available original elastic scattering experimental data reported by other groups.[13−18] Their angular dispersion trends as shown in Fig. 2 are deduced from the original experimental data of differential cross section angular distribution for the halo nuclei ^{6}He at 29.6 MeV and 27 MeV respectively, stable nuclei ^{6}Li at 73.7 MeV and 99 MeV respectively, ^{16}O at 170 MeV and ^{4}He at 40 MeV on target ^{208}Pb.

For all of the six reaction systems shown in Fig. 2, there are two straight lines to fit the experimental data with two different slopes in the angular dispersion plane of $\ln(d\sigma/d\theta)$ vs θ^2. We call the angle as an angular dispersion turning angle θ_{tu} corresponding to a turning point of two different slopes. As listed in Table 1, the θ_{tu} is at forward angular range within the grazing angle θ_{gr} of the reaction system. The ratio between the θ_{tu} and the θ_{gr} are reduced about 0.20 for the halo and/or weakly bound nuclei and increase about 0.44 for the stable nuclei.

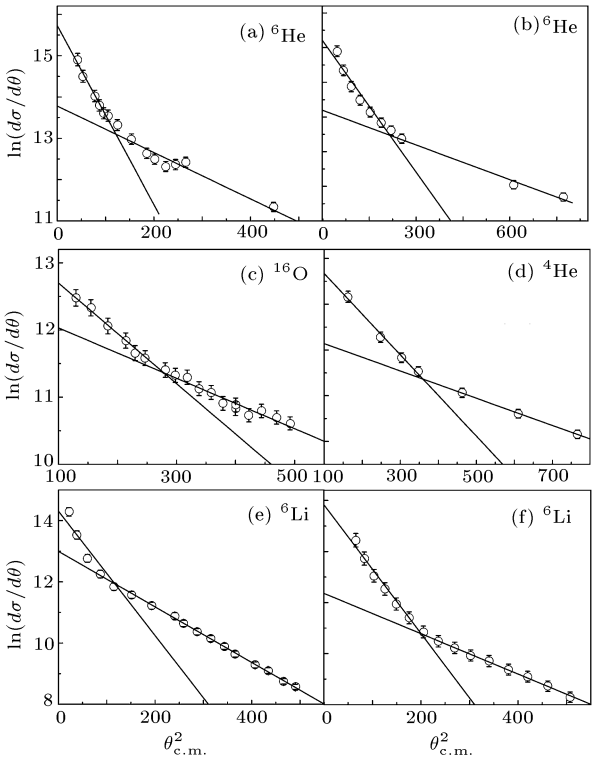

Fig. 2. Angular dispersion plots of $\ln(d\sigma/d\theta)$ vs θ^2 in the c.m. system for elastic scattering products of (a) ^{6}He, (b) ^{6}He, (c) ^{16}O, (d) ^{4}He, (e) ^{6}Li and (f) ^{6}Li.

In the following we present a understanding of the angular dispersion turning angle based on a classical picture of deflection function in heavy ion collisions. The classical deflection angle θ as a function of the impact parameter b can be written[1−3] as

$$\Theta(b) = \pi - 2\int_0^{b/r_{\min}(b)} {\rm d}w\Big(1 - \frac{V[r(w)]}{E} - w^2\Big)^{1/2}, \quad (4)$$

with

$$r(w) = b/w. \quad (5)$$

The distance of closest approach $r_{\min}(b)$ can be obtained from energy and angular momentum conservation. For a given incident energy E, the deflection angles $\theta(b)$ are determined by the potential $V(r)$. The first important step to calculate the deflection function is to structure a proper effective heavy ion interaction potential $V_{\rm eff}(r)$ quantitatively. Supposing $V_{\rm eff}(r) = V_N(r) + V_{\rm Clb}(r)$, in addition to the Coulomb potential $V_{\rm Clb}(r)$, a nuclear potential $V_N(r)$ is usually assumed to be attractive. For all of the reaction

system we discussed in this study, the incident energies E are greater than the critical energy $E_{\rm crit}$, this means that in our case there are both the Coulomb rainbow angle and nuclear rainbow angle in the trajectory of the classical deflection function, as shown in Fig. 3.[1−3,21] By the way, as the classical trajectory leading to the Coulomb rainbow only grazes the nuclear surface, the Coulomb rainbow angle θ_1 is close to the grazing angle θ_{gr}.[22]

Table 1. Turning point angle θ_{tu} of the angular dispersion in heavy ion elastic scattering.

Reaction System	$E_{\rm lab}$	$E_{\rm c.m.}/V_{CB}^{\rm a}$	$\theta_{gr}^{\rm b}$	Angular range detected	θ_{tu}	θ_{tu}/θ_{gr}	Projectile nucleus	
^{17}F+^{208}Pb	141 MeV	1.5	59°	6 −20°	12°	0.20	Weakly bound	Our work
^{17}O+^{208}Pb	128 MeV	1.5	57°	6 −20°	$>21°$	>0.37	Stable	Our work
^{6}He+^{208}Pb	29.6 MeV	1.4	60°	$>6°$	11°	0.18	Halo	Ref. [13]
^{6}He+^{208}Pb	27 MeV	1.3	72°	$>6°$	15°	0.21	Halo	Ref. [14]
^{16}O+^{208}Pb	170.1 MeV	2.0	38°	$>11°$	17°	0.45	Stable	Ref. [15]
^{4}He+^{208}Pb	40 MeV	1.9	43°	$>12°$	19°	0.44	Stable	Ref. [16]
^{6}Li+^{208}Pb	73.7 MeV	2.3	33°	$>8°$	14°	0.42	Stable	Ref. [17]
^{6}Li+^{208}Pb	99 MeV	3.1	22°	$>5°$	10°	0.45	Stable	Ref. [18]

[a]Coulomb barrier calculated as discussed in Ref. [19].

[b]Grazing angle values taken from the experimental data or calculated by non-relativistic kinematics, see Ref. [20].

Table 2. Optical potential parameters of different reaction system.

Reaction System (+208Pb)	$E_{\rm c.m.}$ (MeV)	$E_{\rm lab}$	Potential parameters						χ^2
			Real			Imaginary			
			V0	R0	a	W	Rw	Aw	
^{17}F	130	141	535	2.2	2.23				
^{6}He	28.75	29.6	22.4	7.4	1.25				
^{6}He	26.22	27	29	6.7	1.38	6.494	8.3	1.675	0.0573
^{16}O	157.8	170.1	122	6.2	1.42	6.12	11.3	0.68	0.584
^{4}He	39.24	40	20.2	7.05	1.04	3	11.57	0.246	0.524
^{6}Li	96.19	99	36.5	6.4	1.06	6.61	11.24	0.644	0.636
^{6}Li	71.61	73.7	36.6	6.55	1.13	5.125	11.57	0.552	0.191

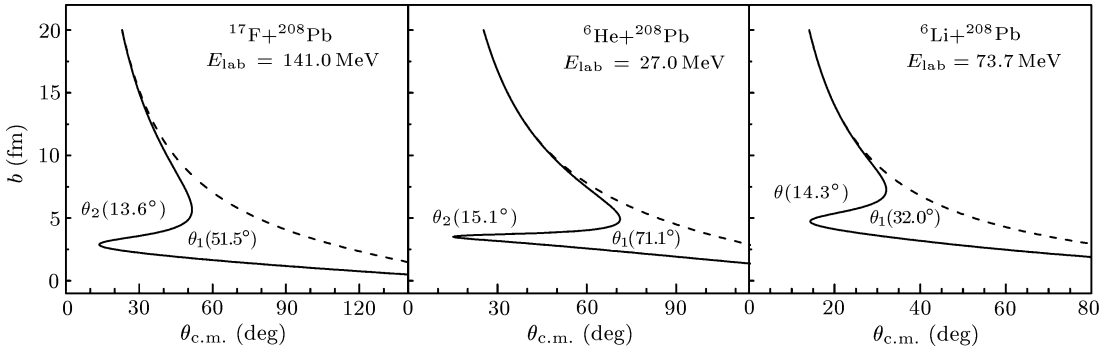

Fig. 3. Typical Classical deflection function results.

In addition, in the view of the dimension of scattering angle in the classical deflection function, for those elastic scattering products emitted in forward angles much smaller than the nuclear rainbow angle θ_2 as shown in Fig. 3, there is only the Coulomb interaction. As soon as the scattering angle have increased to larger than θ_2, there are two interaction potentials, nuclear and Coulomb, so that the point at θ_2 is a turning point of different reaction mechanisms, a pure Coulomb scattering and an elastic scattering with nuclear interaction. This is consistent with the slope change due to the contribution from the dynamic angular dispersion with nuclear interaction in the angular dispersion plot as shown in Figs. 1 and 2. This is to say, the angular dispersion tuning angle θ_{tu} in Figs. 1 and 2 corresponds just to the nuclear rainbow angle θ_2 in Fig. 3.

Nevertheless in our experimental measurement, the angular dispersion of elastic scattering products of ^{17}O on target ^{208}Pb are approximately on a straight line as shown in Fig. 1, there is no angular dispersion turning angle observed. This is because too limited forward angular range less than 20° is measured in the experiment and θ_{tu} for 128 MeV ^{17}O+^{208}Pb is predicted about 25° by the systematic analysis listed in Table 1.

In our calculations to the classical deflection function, a real Woods–Saxon type is taken as our nuclear potential. In order to eliminate the uncertainty of the potential parameters, three quantities are used as a

set of criteria: the grazing angle θ_{gr} as the Coulomb rainbow angle, the angular dispersion turning angle θ_{tu} as the nuclear rainbow angle and the critical angular momentum L_{cr} as another limitative condition. As typical examples, Fig. 3 presents three calculation results of the classical deflection function. The related real potential parameters for all the seven reaction systems listed in Table 1 are given in Table 2. In comparison of these potentials used in the calculation of the classical deflection function, there are obvious more diffuseness for the halo nucleus ^{6}He as projectiles than ordinary ones of ^{6}Li and ^{4}He, and for the weakly bound nucleus ^{17}F than the stable ^{16}O. It is still fortunate that these potential parameters are unique in the calculation to the deflection function for a fixed reaction system with the three limitative conditions θ_{gr}, θ_{tu} and L_{cr} motioned above. If these three limitative conditions are reasonable, then it should be reflected by a positive result to fit the differential cross sections of elastic scattering.

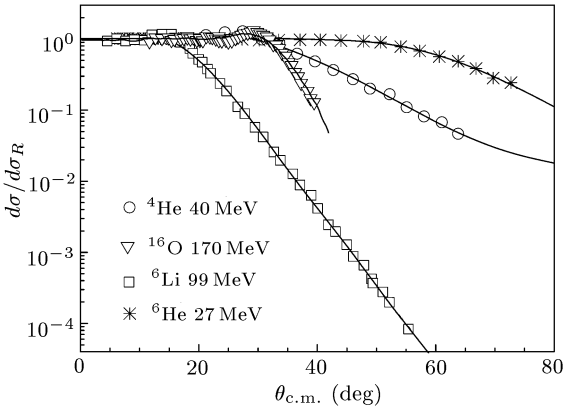

Fig. 4. Fit to the differential cross sections of elastic scattering products by FRESCO code.

The differential cross sections of these elastic scattering data have been fitted with the search version of computer code FRESCO[23] using the optical model, where the real parts were fixed using the results of the analysis of the classical deflection functions, as is listed in Table 2, and three parameters of the imaginary parts of a Woods–Saxon form are varied to fit the experimental data. Very good fittings are obtained, as shown in Fig. 4 for scattering of ^{4}He, ^{6}Li, ^{16}O and ^{6}He at 27 MeV. The resulting parameters of the imaginary parts are listed in Table 2 with their related χ^2 values. The χ^2 values are calculated by assuming a uniform error of 10% of the experimental data. The elastic scattering data of ^{17}F and ^{6}He at 29.6 MeV could not be fitted using such a simple optical model, maybe because higher order effects, such as the coupling to the breakup channels, play an important role in their scattering processes and require more sophisticated analysis, such as those in Ref. [13].

In summary, differential cross sections for elastic scattering products of ^{17}F on ^{208}Pb at 141 MeV has been measured at $\theta_{\rm lab}$ from 6° to 20°. The angular dispersion plot of $\ln(d\sigma/d\theta)$ versus θ^2 is obtained from the angular distribution of the elastic scattering differential cross sections. Systematic analysis on the angular dispersions has been performed by using classical deflection function of elastic scattering for the available experimental data. The results indicate that: (1) The nuclear rainbow angle for such reaction systems can be determined by measuring differential cross sections of elastic scattering at forward angular range and analysing the angular dispersion. (2) There is an exotic behaviour, smaller angular dispersion turning angle and more diffuseness in the nuclear potential, for the halo nuclei as the projectiles in elastic scattering. (3) Analysis of angular dispersion may provide a way to determine a set of reasonable optical potential parameters to fit the experimental data of elastic scattering differential cross sections.

We thank Wang Shunjin for his suggestion and fruitful discussion.

References

[1] Nörenberg W 1980 Basic concepts in the description of collisions between heavy nuclei in *Heavy Ion Collisions* ed Bock R (Amsterdam: North-Holland) vol 2 pp 1–43
[2] Frahn W E 1984 *Elastic Scattering* in *Treatise on Heavy-Ion Science* ed Bromley D A (London: Plenum) vol 1 pp 135–290
[3] Hu J M 1996 *Nuclear Theory* (Beijing: Atomic Energy Press) vol 2 p 265 (in Chinese)
[4] Wang Q et al 2006 *Chin. Phys. Lett.* **23** 1731
[5] Strutinsky V M 1973 *Phys. Lett.* B **44** 245
[6] Abul-Magd A Y et al 1979 *Phys. Lett.* B **83** 27
[7] Gobbi A and Nörenberg W 1980 Dissipative collisions in it Heavy Ion Collisions ed Bock R (Amsterdam: North-Holland) vol 2 pp 127–274
[8] Rosa A De et al 1989 *Phys. Rev.* C **40** 627
[9] Rosa A De et al 1990 *Phys. Rev.* C **41** 2062
[10] Rosa A De et al 1991 *Phys. Rev.* C **44** 747
[11] Wang Q et al 2004, *Chin. Phys. Lett.* **21** 1911
[12] Dong Y C, Wang Q, Li S L et al 2005 *High Energy Phys. Nucl. Phys.* **29** 147
[13] Rusek K, Keeley N, Kemper K W and Raabe R 2003 *Phys. Rev.* C **67** 041604R
[14] Kakuee O R et al 2003 *Nucl. Phys.* A **728** 339
[15] Baker S D and Mcintyre J A 1967 *Phys. Rev.* **161** 1200
[16] Perry R et al 1981 *Phys. Rev.* C **24** 1471
[17] Huffman R, Galonsky A, Markham R and Williamson C 1980 *Phys. Rev.* C **22** 1522
[18] Schwandt P, Jacobs W W, Kaitchuck M D and Singh P P 1981 *Phys. Rev.* C **24** 1522
[19] Huizenga J R 1977 *USERDA Progress Reprot COO-3496-65* p 131
[20] Marion J B 1968 *Nuclear Reaction Analysis* (Amsterdam: North-Holland)
[21] Khoa D T et al 2007 *J. Phys.* G **34** 111
[22] Dasilveira R 1973 *Phys. Lett.* B **45** 211
[23] Thompson I J 1988 *Comput. Phys. Rep.* C **7** 167